Proceedings of 2004 Korea-Japan Joint Seminar
on Particle Image Velocimetry
POSTECH, Korea, Dec. 9 - 10

Analysis of Flow around a Rotating Marine Propeller using PIV Techniques

Sang Joon Lee and Bu Geun Paik

Mechanical Engineering,
Pohang University of Science and Technology,
San 31, Hyo-Ja Dong, Pohang, Korea
sjlee@postech.ac.kr

Abstract: The characteristics of flow around a rotating propeller were investigated using PIV technique. For each of four different blade phases of 0°, 18°, 36° and 54°, four hundred instantaneous velocity fields were ensemble averaged to investigate the spatial evolution of the flow around a propeller. The phase-averaged mean velocity fields show that the viscous wake formed by the boundary layers developed on the blade surfaces and the slipstream contraction in the near-wake region. The out-of-plane velocity component and strain rate had large values at the locations of the tip and trailing vortices. The boundary layer developed along the ship hull bottom surface of the ship stern provides a strong turbulent shear layer, affecting the vortex structure in the propeller near-wake. As the flow develops in the downstream direction, the trailing vortices formed behind the propeller hub move upward slightly due to the presence of the hull wake and free surface. The turbulence intensity has large values around the tip and trailing vortices. As the wake moves downstream, the strength of the vorticity diminishes and the turbulence intensity increases due to turbulent diffusion and active mixing between the tip vortices and adjacent wake flow.

Keywords: PIV, Propeller wake, Tip vortex, Free surface

1. Introduction

As marine vehicles become larger and faster, loading on the propeller blades becomes higher. The increase of propeller loading may cause problems such as noise, hull vibration, and cavitation at high speed. Especially, tip and hub vortices of propeller wake may reduce the propulsion efficiency and generate rudder cavitation that can be source of corrosion or erosion on rudder surface. In order to avoid these problems, the geometry of modern propeller becomes to have more complicated shape. In addition, a marine propeller is influenced by hull wake because the propeller is attached to the ship hull. Since the propeller is located at a relatively shallow depth, it is also affected by free surface. Therefore, the detail inflow and wake analysis based on reliable experimental data is essential to optimize the geometrical shape of a propeller.

The flow around a marine propeller has been investigated numerically using many different kinds of numerical schemes. Kerwin (1978) predicted the steady and unsteady propeller performance with lifting surface theory. However, the lifting surface theory does not predict accurately the flow around the leading edge and blade tips. Lee (1987) and Kim et al. (1993) used the potential-based panel method to predict the steady performance of a propeller. A further improvement was made by Cho and Lee (2000) by applying the B-spline higher-order panel method to obtain more accurate numerical results. Some numerical attempts based on either potential or

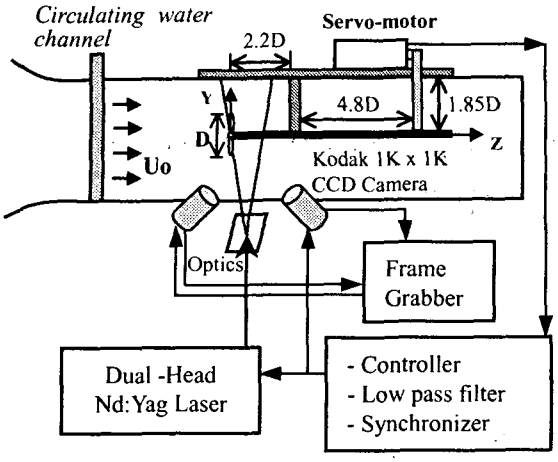

Fig. 1 SPIV and coordinate system

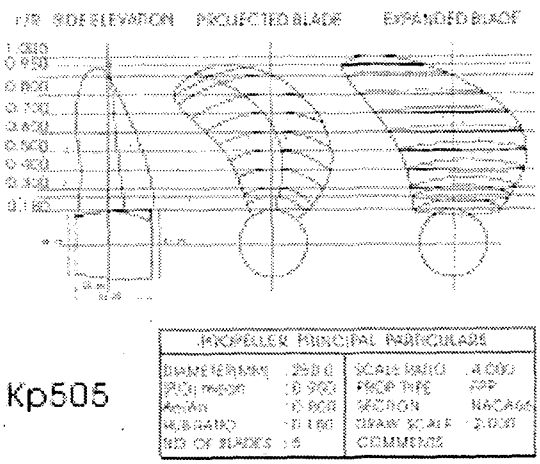

Fig. 2 Geometry of KP505 propeller

viscous flow model have been tried to yield satisfactory predictions of the formation and trajectory of tip or trailing vortices. However, these numerical analyses require adequate wake sheet modeling based on reliable experimental data or specified theory. In addition, it is very important to predict the strength and trajectory of the tip vortices that cause energy loss in propulsion, hull vibration and noise. The vortex sheet of wake has been assumed as a thin filament in numerical analysis.

The flow around a propeller has been usually investigated using point-wise techniques such as hot-film, Pitot tube and LDV (Laser Doppler Velocimetry), measuring velocities at discrete points by traversing the flow sensors. For example, Stella et al. (1998) measured the axial velocity of a propeller wake, and investigated the tip vortex using an LDV system. However, point-wise techniques measure velocity vectors sparsely and LDV needs substantial time to investigate flow in a whole measurement plane.

Recently, particle image velocimetry (PIV) was employed to measure the velocity fields of flow behind a rotating propeller attached to a container ship model (Paik et al., 2004). In addition, phase-averaged particle tracking velocimetry (PTV) has been used to measure the characteristics of a propeller wake (Lee et al., 2004a). To further clarify the propeller wake, Lee et al. (2004b) used a stereoscopic PIV (SPIV) technique to measure the three component velocity fields of the wake behind a marine propeller in the longitudinal planes.

The main objectives of present study are to analyze the flow around a rotating marine propeller in detail. The isolated propeller and the rotating propeller attached at KRISO 3600TEU container ship model (hereafter, KCS) were tested in this study. The spatial distributions of the mean velocity and turbulence statistics of the propeller wake were elucidated by measuring 400 instantaneous velocity fields at each of four different phases of the propeller blade by using a phase-averaged PIV techniques. The experimental data reported here will provide useful information for the validation of numerical predictions.

2. Experimental apparatus and method

2.1 Isolated Propeller

The stereoscopic PIV (SPIV) system consists of a dual-head Nd:YAG laser, two Kodak two-frame CCD cameras, a synchronizer, and an IBM PC, as shown in Fig. 1. The Nd:YAG laser has a pulse width of about 7 ns with a pulse energy of 125 mJ for each head. The two CCD cameras, which are installed at an angle of 50.8°, each capture a particle image of spatial resolution 1024 × 1024 pixels. The CCD cameras and laser were synchronized with the angular position of the propeller blade.

The circulating water channel in which the propeller wake was measured had a test section

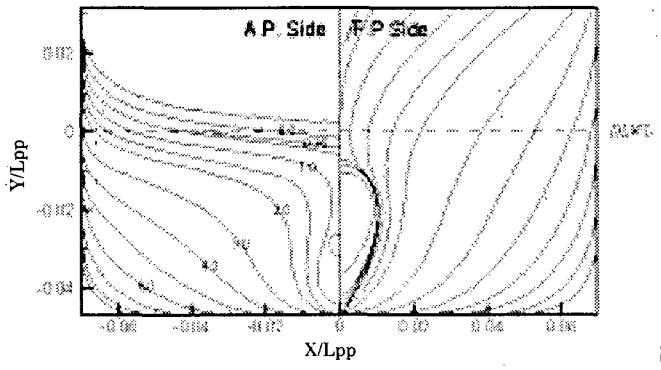

Fig. 3 Body plan of KRISO 3600TEU container ship

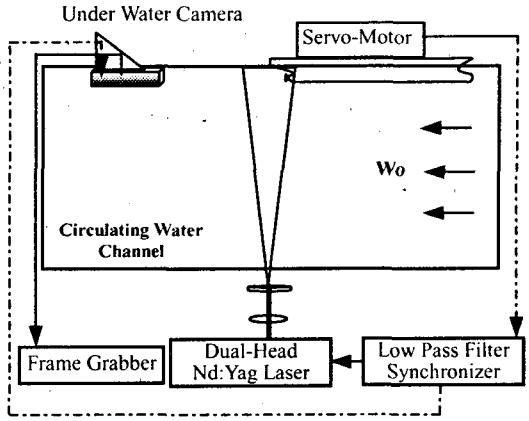

Fig. 4 Experimental set-up

size of $120^{L} \times 30^{W} \times 20^{H}$ cm^3. Figure 2 shows the KP505 propeller for the KRISO 3600TEU container vessel tested in present study. The KP505 propeller has 5 blades with a design advance ratio J(= V_a/(nD)) of 0.72. Here, V_a is the advance velocity, n is the rotational frequency and D is the propeller diameter. For the KP505 propeller, the propeller diameter is 54 mm and the hub ratio is 0.18. The uniform free stream velocity was fixed at 32.5 cm/s and the Reynolds number based on the propeller diameter is about 18,000. The measurement plane was illuminated from the bottom of the water channel with a thin laser light sheet of thickness 3 mm and the field of view was 6×6 cm^2. Silver-coated hollow glass beads of mean diameter 10 μm were used as seed particles.

The angular-type camera arrangement used in the present SPIV system was carefully calibrated so as to minimize errors due to any image distortion or non-uniform magnification created by the tilted image planes and camera lenses, thereby ensuring accurate flow field data. Three-dimensional velocity components (axial velocity component u, vertical velocity component v, and out-of-plane velocity component w) were deduced from two sets of consecutive particle images captured from the left and right cameras of the SPIV system. In the experiments, 24×24 pixels interrogation windows overlapping by 50% were used to obtain instantaneous velocity fields from the particle images captured by each CCD camera.

Four hundred instantaneous velocity fields were obtained for each measurement phase. The time-averaged in-plane and out-of-plane velocity distributions, vorticity distribution, strain rate distribution and turbulence characteristics such as turbulence intensity were obtained by ensemble-averaging the instantaneous velocity fields in order to investigate the spatial evolution of the wake structure.

2.2 Propeller attached to ship model

The two-frame PIV system with the CCD camera of 1024×1024 pixels was employed to investigate the wake behind a rotating propeller attached to a KRISO 3600TEU container ship model. The experimental model was installed in a circulating water channel of test section size $4.5^{L} \times 1.0^{W} \times 1.0^{H}$ m^3. To generate the fully developed turbulent boundary layer, a trip-wire device was used on the ship model. Figure 3 shows the body plan of the KCS.

The free stream velocity (W_0) was fixed at 0.6 m/s and the corresponding Froude number is 0.16. The revolution speed of the propeller corresponding to the design advance ratio of J = 0.72 is 15.43 rps (revolutions per second). The Reynolds number based on the length between perpendiculars of the ship is about 9×10^5. The wake was illuminated from the side of the water channel with a laser light sheet of about 2 mm in thickness with a field of view of 6×6 cm^2.

The CCD camera was installed in a watertight housing to capture particle images directly, thereby avoiding image distortion. The CCD camera had a long-focal-length lens attached and was placed 0.9 m downstream of the propeller plane. This setup ensured that the distance between the camera housing and the propeller was sufficiently long to avoid interference effects caused by the camera housing. Figure 4 shows the definition of coordinate system and the positions of the measurement planes.

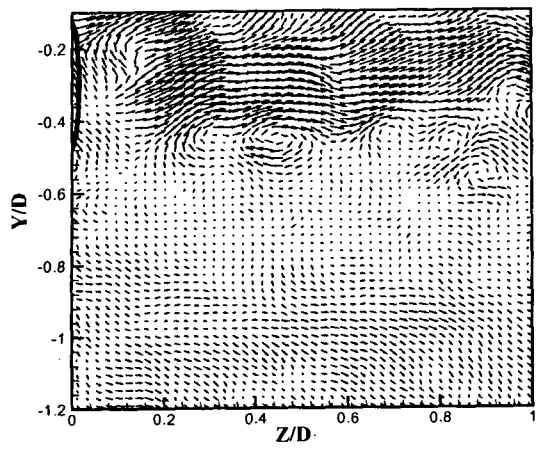

Fig. 5 Instantaneous velocity fluctuation at ϕ = 0°

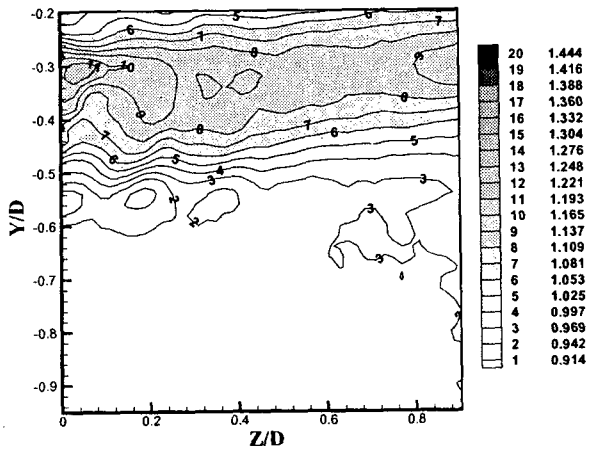

Fig. 6 Contour plots of phase-averaged axial velocity at ϕ = 0°

3. Results and discussion

3.1 Isolated Propeller

Figure 5 shows the instantaneous velocity field subtracted by W_0=32.5 cm/s at the phase angle of ϕ = 0°. The periodic wake sheets and tip vortices in the clockwise rotation are shed successively from the blade tips with a regular interval are clearly seen.

The contour plots of phase-averaged axial velocity at ϕ = 0° are shown in Fig. 6. The axial velocity component has relatively small values in the blade tip and propeller shaft. The viscous wake indicating the defects of axial velocity component appears in the near-wake region due to the merging of two boundary layers developed on both sides of propeller blade surfaces. On the average, the viscous wake has minimum values around 0.7R of the propeller blade span where R is the propeller radius. This agrees well with the propeller design that assigns the maximum loading around 0.7R.

Figure 7 shows the contours of phase-averaged vorticity at ϕ = 0°. A trailing vortex generated from the pressure difference between upper and lower surfaces of a propeller blade rolled up from a vortex sheet. The tip vortices evolve downstream with a regular spacing periodically. The trailing vortices called as the potential wake are originated from the trailing edge of the propeller blade. The trailing vortices are composed of two vorticity layers with a positive or negative sign, which are developed on the blade surfaces and the vortex exists between these two layers. The tip vortex has a strong asymmetry shape in the initial wake region up to Z/D = 0.3. The asymmetry of tip vortex was caused by the interaction between tip vortex and wake sheet. As the flow goes downstream, the asymmetry turns to symmetry as the tip vortices are separated from the wake. Tip vortex has a concentric circles shape, while the trailing vortices have the curled shape toward the propeller shaft from the tip.

The out-of-plane velocity component (u) distribution was measured to investigate the out-of-plane motion of the wake structure. The out-of-plane velocity component has large values along the trailing vortices. The present observation of non-axial flow motion of the wake indicates that all of the propulsion energy is not consumed effectively. Therefore, measurements of the out-of-plane velocity component together with the strength of the tip vortices such as those presented here could be used to guide the design of more effective marine propellers.

3.2 Propeller attached to ship model

The flow following the hull surface cannot sustain the rapid change of curvature around the

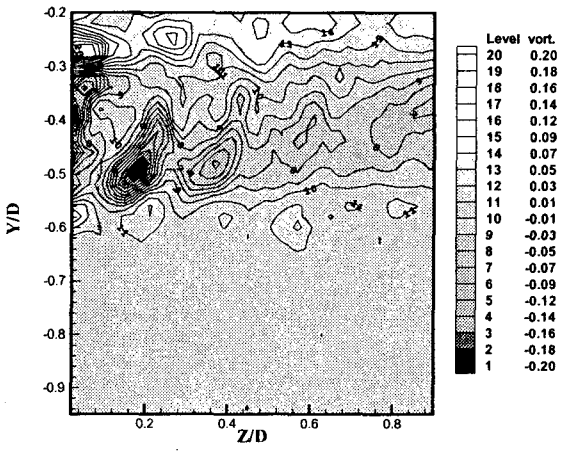

Fig. 7 phase-averaged spanwise vorticity at ϕ = 0°

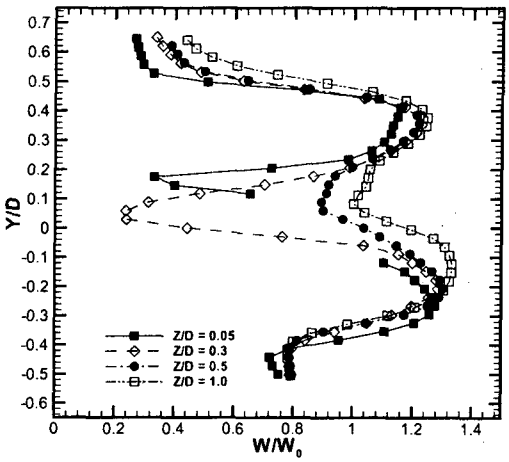

Fig. 8 Variation of axial velocity profiles at several downstream locations at ϕ = 0°

bilge and separates in the stern region. The fluid inside the boundary layer moves away from the hull and is replaced with outside inviscid fluid via large-scale bilge vortices. The bilge vortices are composed of two vortices, one rotating counterclockwise with positive vorticity and another rotating clockwise with negative vorticity. The bilge vortices that develop along the hull surface enter the propeller plane and directly influence the propeller wake.

The axial velocity component has relatively small values in the vicinity of the blade tip and propeller hub. Velocity deficit dominates the region around the blade tip, especially near the free surface. Near the wake center (Y/D ≈ 0.2), velocity deficit dominates in the region just behind the propeller (Z/D < 0.3) but vanishes rapidly thereafter, as shown in Fig. 8.

The axial velocity in the upper slipstream region (Y/D > 0) is about 10% smaller than that in the lower slipstream region (Y/D < 0), which is influenced by the hull wake. With going downstream, the slipstream tube is shifted gradually upward due to the presence of the free surface. In the water close to the air-water interface, coupling between the free surface and the wake behind the ship hull retards the axial velocity component of the propeller wake. This complicated flow interaction deforms the velocity profile behind the propeller up to one propeller diameter downstream. It is interesting to note that the velocity profile in the lower slipstream resembles that of an isolated propeller wake, indicating that the free surface has little influence on this region of the wake. The contraction slope of the lower slipstream is also much larger than that of the upper slipstream.

Figure 9 shows a contour plot of the phase-averaged spanwise vorticity(ω_x) in the longitudinal plane at ϕ = 0°. The tip vortices are continuously generated from the propeller blade tip in the slipstream, and the trajectory of these vortices seems to move slightly toward the propeller axis in the downstream region. The trailing vortices in the lower slipstream consist of two types of vorticity layers originating from the two surfaces of propeller blade, one of positive vorticity and the other of negative vorticity. In the upper slipstream, the trailing vortices with negative vorticity are stronger than that with positive vorticity. The trailing vortices in the upper slipstream are deformed highly, compared with those in the lower slipstream. The slow and non-uniform incoming flow in the upper slipstream seems to lead to the formation of a complicated vortex structure behind the propeller and brings about insufficient momentum in the axial direction. Downstream of Z/D = 0.5, the trajectories of the tip vortices expand and fluctuate due to the interaction with the wake sheets. Each tip vortex is paired with a trailing vortex in close proximity. This relationship between the tip and trailing vortices diminishes gradually as the wake goes downstream due to the fact that the advance speed of the slipstream is faster than that of the tip vortices.

Figure 10 shows the trajectories of the tip vortices in the lower slipstreams for four phase angles. There is no significant variation with respect to the phase angle up to Z/D = 0.8, however, large variation of trajectories starts from the downstream over Z/D = 1.0 where the wake structure becomes unstable. In the lower slipstream region, the tip vortices appear at regular intervals (~0.15D in the Z direction) up to the downstream location of Z/D = 0.5. This trend is similar to that observed for an isolated propeller (Lee et al., 2002). Downstream of Z/D = 0.5, tip vortices moves

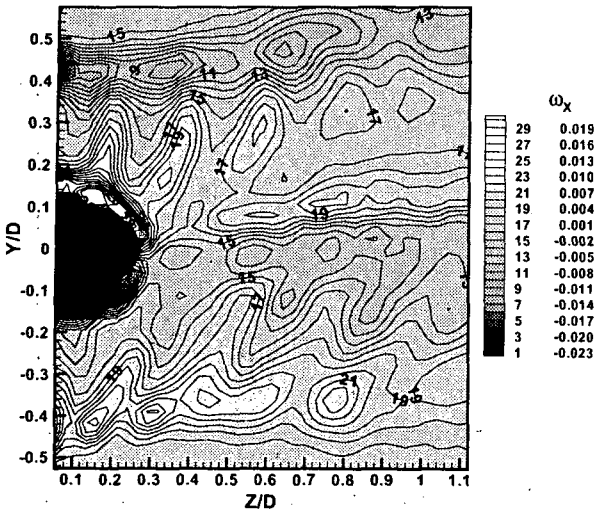

Fig. 9 Phase-averaged spanwise vorticity(ω_x) at ϕ = 0°

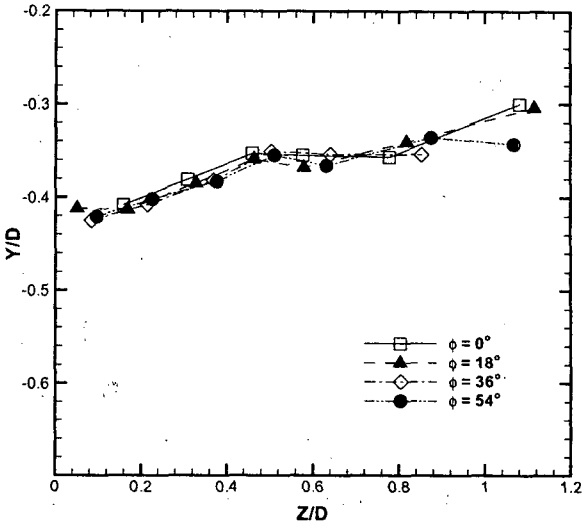

Fig. 10 Trajectories of tip vortices in the lower slipstream

downstream with about 0.2D interval. The oscillatory behavior observed near Z/D =0.5 and the break-up of the periodic vortex structure in the region downstream of Z/D = 0.5 seems to be caused by blade-to-blade interactions and slow marching tip vortices .

Figure 11 shows contour plots of the phase-averaged streamwise vorticity(ω_z) at ϕ = 0° and 54°. In the transverse plane of Z/D = 0.3, the slipstream of the propeller wake is slightly contracted and the tip vortices are located at r ≈ 0.9R (where R is the radius of propeller). The tip and trailing vortices rotate clockwise with increasing phase angle. The tip vortices have positive vorticity. In contrast, the trailing vortices are composed of two vorticity layers of opposite sign. In particular, the region of negative vorticity in the trailing vortices come into contact with the region of positive vorticity at around r = 0.7R. This coincides with the design concept of the KP505 propeller, which aims to place the maximum loading at around r = 0.7R. The vorticity fields shown in Fig. 11 give information on the radial distribution of the loading on the blades. It is clear from these vorticity fields that each blade has a different loading distribution due to the non-uniformity of the incoming flow.

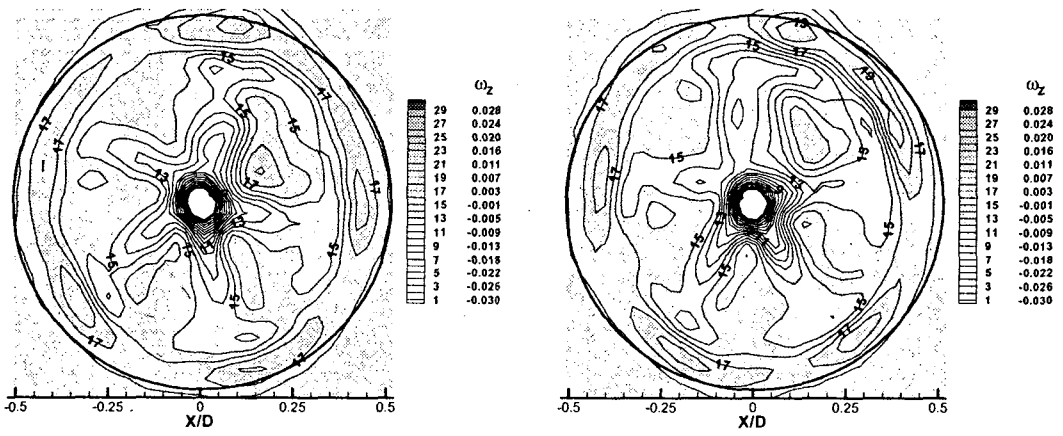

(a) ϕ = 0° (b) ϕ = 54°

Fig. 11 phase-averaged streamwise vorticity at Z/D = 0.3

6. Conclusion

The complicated 3-D flow structure of the turbulent wake behind the isolated propeller was investigated experimentally using SPIV technique. A viscous wake displaying velocity deficits was clearly observed in the region near the blade tip. As the flow moved downstream, the traces of the tip vortices contracted toward the propeller shaft up to X = 0.5D and thereafter oscillated due to a blade-to-blade interaction. As the wake moved downstream, the strength and skewness of the tip vortices decreased. Strong out-of-plane motion was observed within the propeller slipstream. The out-of-plane velocity beyond the location of the tip vortices was about 8~13% of the free stream velocity in the near-wake region. This large out-of-plane velocity component may be the main source of the perspective errors that lead to overestimation of the in-plane velocity field. Thus, the present results indicate that a SPIV technique that measures the three velocity components will be very useful for the accurate characterization of propeller wakes with strong out-of-plane motions.

The flow characteristics of the wake behind a rotating propeller attached to a KRISO 3600TEU container ship model were investigated using a two-frame PIV technique. Phase-averaged mean velocity fields in the longitudinal and transverse planes were obtained. The retarding effect of the hull wake on the propeller wake delays the marching of the tip vortices in the longitudinal plane. The inflow velocity and bilge vortices developed along the hull affect the radial and tangential velocity profiles of the propeller wake. After the location of Z/D = 0.5, the vortices decrease in strength; however, the turbulence intensity increases due to turbulent diffusion and active mixing with the surrounding fluid. Collectively, the present results demonstrate that the propeller wake has a complicated 3-D flow structure that is quite different from that of the isolated propeller, and is substantially influenced by the hull wake.

Acknowledgement

The present work was supported by the National Research Laboratory Program of Ministry of Science and Technology (MOST) of Korea.

References

Cho, C.H. and Lee, C.S., "Numerical Experimentation of a 2-D B-Spline Higher Order Panel Method," J. of SNAK, 37(3), (2000) 27-36.

Kerwin, J.E. and Lee, C.S., "Prediction of steady and unsteady marine propeller performance by numerical lifting surface theory," Transaction of SNAME, 86, (1978) 218-253.

Kim, Y.G., Lee, J.T., Lee, C.S., and Suh, J.C., "Prediction of steady performance of a propeller by using a potential-based panel method," Trans. of SNAK, 30(1), (1993) 73-86.

Lee, J.T., "A potential-based Panel Method for the Analysis of Marine Propellers in Steady Flow," Ph.D. Thesis, Dept. of Ocean Engineering, M.I.T., Mass. (1987)

Lee, S.J., Paik, B.G. and Lee, C.M., "Phase-averaged PTV Measurements of Propeller Wake," J. of Ship Research, (2004a) accepted

Lee, S.J., Paik, B.G., Yoon, J.H. and Lee, C.M., "Three Component Velocity Field Measurements of Propeller Wake Using Stereoscopic PIV Technique," Exp Fluids, 36(4), (2004b) 575-585.

Paik, B.G., Lee, C.M. and Lee, S.J., "PIV Analysis of Flow around a Container Ship Model with a Rotating Propeller," Exp Fluids, 36(6), (2004) 833-846.

Stella, A., Guj, G., Di Felice, F., and Elefante, M., "Propeller Wake Evolution Analysis by LDV," Proceedings of 22nd Symposium on Naval Hydrodynamics, Washington D.C., (1998) 171-180.